Study on the Fluid Dynamics of Bottle Emptying

Shenglin Yue[1,*], Xiaotian Dong[2], Rongtian Na[3], Zhixin He[4]
{sy3u24@soton.ac.uk[1], dongxt@jou.edu.cn[2],
rongtian.na@mail.utoronto.ca[3], hezhx28@mail2.sysu.edu.cn[4]}

University of Southampton, School of Ocean and Earth Science, Southampton, United Kingdom[1]
Jiangsu Ocean University, School of Civil and Ocean Engineering, Lianyungang, China[2]
University of Toronto, St. George Campus, Department of Earth Science,
Department of Mathematics, Toronto, Ontario, Canada[3]
Sun Yat-Sen University, Department of Civil Engineering, Zhuhai, China[4]
*corresponding author

Abstract. The bottle pouring phenomenon has been studied due to its complex process and unique industrial value. This study, based on pouring experiments with six different bottles, discovered a strong quadratic relationship between emptying time and the inclination angle. The findings of Clanet and Serby were refined, resulting in an equation for emptying time that accounts for variations in inclination angle. The emptying process of the bottle can be divided into two stages: the bubble stage and the flow stage. It was observed that as the inclination angle increases, the "bubble stage" occupies a longer duration. Combining experiments and CDF, the exponential relationship between the relative maximum flow rate and the relative bottle mouth diameter was obtained by regression method.

Keywords: Emptying bottle, Fluid dynamics, CFD

1 Introduction

The way a liquid is in a bottle, which we often encounter daily performing actions as basic as pouring drinks into glasses, empties require a complicated interplay between the gas and liquid phases known as the "glug-glug" effect. This effect is known for a unique periodic acoustic signature of liquid egress counterposed with air bubble Ingres. A detailed study of this process would direct to industrial applications such as optimizing container designs.

Studying the "glug-glug" effect will better interpret container water flow and understand fluid mechanics. These flow patterns observed during the emptying process of an ideal verticle bottle were first investigated by Clanet and Serby in 2004 [1], based on the experimental result of Davis and Taylor (1988) [2]. A spring-mass analogy model was suggested, describing the duration of emptying in a power-law function with respect to bottle outlet diameter, which affects bottle parameter dimension designs [1].

CONF-CIAP 2025, January 17-23, Eskisehir, Turkey

DOI 10.4108/eai.17-1-2025.2355237

The **Clanet and Searby formula** expresses the predicted emptying time T_e relative to the unrestricted emptying time T_{e0} as:

$$\frac{T_e}{T_{e0}} = \left(\frac{D_0}{d}\right)^{5/2} \tag{1}$$

where D_0 is the diameter of the tube and d is the diameter of the outlet. This relationship indicates that the emptying time increases with the ratio D_0/d, due to the greater challenge in synchronizing air ingress and liquid egress.

This time, an experimental study was conducted by Kenton, Neufeld, and Huppert (2012) investigating the impact of physical parameters on the emptying process, mainly focusing on the diameter of the bottleneck or shape type for different liquid properties. The results suggest a clear relationship between bottle geometry (the shape), flow angle (tilt), and exit diameter with respect to how fast the emptying process is. The study finds the best incline angle and outlet diameter to reduce emptying time, which applies to industry designs [3].

The **Hans C. Mayer formula** quantifies the emptying process, stating that the emptying time T_e is related with the volume V of the bottle and the outlet diameter d [4]. It is represented as:

$$T_e\sqrt{\frac{g}{d}} = (3.8 \pm 0.4)\left(\frac{V}{d^3}\right)^{(0.90\pm0.02)} \tag{2}$$

where g represents the acceleration due to gravity. The formula highlights that a larger bottle volume relative to the outlet size results in a longer emptying time, highlighting the significant role of bottle geometry in fluid discharge.

Mer et al. (2019) conducted more investigation of emptying dynamics in a study. Their study found that the larger neck diameter ratio, losses faster with decreased emptying time, and vice versa at a higher initial fill ratio. [5].

The **Whalley formula** provides a comprehensive model by considering the densities of both the liquid (ρ_L) and gas (ρ_G) phases [6]. The emptying time T_E is given by:

$$T_E = \left(\frac{\left(\rho_G^{1/4} + \rho_L^{1/4}\right)}{[(\rho_L - \rho_G)gd]^{1/4}}\right)^2 \left(\frac{4V}{\pi d^2 C^2}\right) \tag{3}$$

where C is the Wallis constant (0.9 to 1). This formula produces veridical predictions for a subtle view of the interaction between liquid and gas phases during emptying.

Recently, Rohilla and Das (2020) divided the emptying process of the bottles vertically according to the flow characteristics of the bottle emptying process, and found that parameters such as the rising rate of the bubbles at the bottle mouth were affected by the inclination angle and the viscosity of the emptying liquid. At the same time, the main influence of the evacuation process was determined by quantifying the *Re* number and the *We* number [7].

Computational Fluid Dynamics (CFD) analysis can handle complex hydrodynamic phenomena involving multiple phase flows [8]. Schwefler (2021) continued with this analysis, including open, closed, and inverted bottle types. The transition from jetting to bubbling flow started under high

liquid pressure during this process. When the liquid level started dropping, bubbles became apparent, and the flow converted into a bubbled state. Nevertheless, current CFD simulations were found to need to be more accurately distinguishing this transition phase [9].

These studies cover many aspects and factors that contribute to the formation and kinetics of the ”glug-glug” effect and emptying from bottles.

Despite these improvements, the role of lateral inclination and pitcher shape on emptying under natural contditions, that is during a meal or as part of daily activties has not recived enough consideration. Consequently, the present study was conducted under standard atmospheric pressure (101 kPa) and at a temperature of 24°C.

2 Methodology and Experiment Setup

2.1 Experimental Setup

The experiments were conducted with five different models of glass bottles, which varied in shape, size, and consumption output style. These bottles were chosen to cover a variety of geometric variability, which affect the fluid dynamics at the moment within any given pour. The bottles were filled with water to ensure identical initial conditions and placed on an adjustable metal stand. The stand was machined to allow the bottle's inclination angle from vertical upright pouring to tilted pouring at various angles.

The mouth of the bottle, covered with a plastic board, is firmly pressed onto the outlet to apply uniform pressure to start emptying. After the quick removal of this board, flow started with a timer to use at a time when the water was emptied in total.

We conducted a series of seven trials per angle and bottle configuration for each experimental setup to ensure statistical significance. The experiments were conducted in a standard laboratory enviornment with pre-set conditions so that external factors like air currents or temperature changes would not affect the results. The standard error percentage of each bottle per angle was calculated, given by:

$$\delta = \frac{s}{t\sqrt{n}} \tag{4}$$

Where s is the standard deviation of the results, n is the number of trials, and t is the mean of the experimental results. To maintain a standard error margin within 1.5%. The preciseness is a guarantee for the repeatability and accuracy of the results.

Near the system is a high-speed camera, which can record slow-motion video to visualize further how material flows out of it. The formation and behavior of vortices, air bubbles, and liquid streams, as well as a better interpretation of the ”glug-glug” effect, can be seen in videos.

2.2 Experimental Results

2.2.1 Influence of Bottle Shape

In order for the experimental results to reflect the majority of bottle types on the market, the research group conducted multiple experiments using five common glass bottles of different shapes

and sizes. The specific shapes of the bottles are shown in Figure 1. Table 1 provides the characteristic parameters of each bottle and Figure 2 gives an illustration of these parameters.

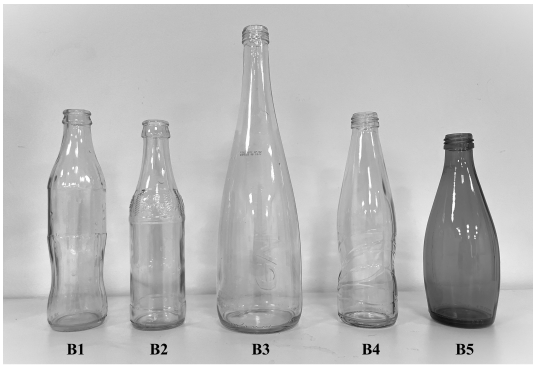

Fig. 1. The five bottles used in the experiment are named B1, B2, B3, B4, and B5 from left to right.

Table 1: Detailed numerical specifications for each bottle.

Bottle	Bottle mouth inside diameter (mm)	Bottle height (mm)	Bottle outer diameter (mm)	Thickness (mm)	Volume (mL)
1	17.0	216	52.8	4.0	296
2	18.0	206	53.5	6.0	275
3	16.7	298	80.0	7.0	800
4	18.0	211	57.6	3.5	300
5	17.2	189	57.3	3.8	355
Graduated Cylinder	49.0	352	53.0	2.0	665

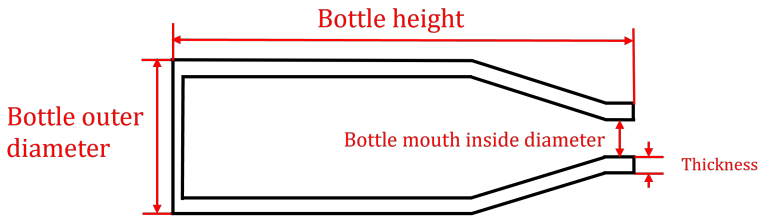

Fig. 2. Diagram of bottle body parameters.

The emptying times of the different bottles at various tilt angles are shown in Figure 2. The results indicate a strong correlation between the bottle mouth diameter and the emptying time. For

B1, B2, and B4, which have similar volumes and shapes, the larger the bottle mouth, the shorter the emptying time at similar tilt angles. Additionally, for the graduated cylinder, which can be equated to a water bottle with a neck and body of equal width, its emptying time is the fastest among all the measured containers, despite having a volume greater than 600 milliliters, much larger than B1, B2, and B4.

Another thing that should be notice is although there are differences in the emptying times among the different bottles, it can be observed that the relationship between bottle tilt angle and emptying time is consistent. Visually, the emptying time of each bottle exhibits a trend of initially decreasing and then increasing. A more in-depth discussion of the effect of tilt angle on emptying time will be provided in section 2.2.2.

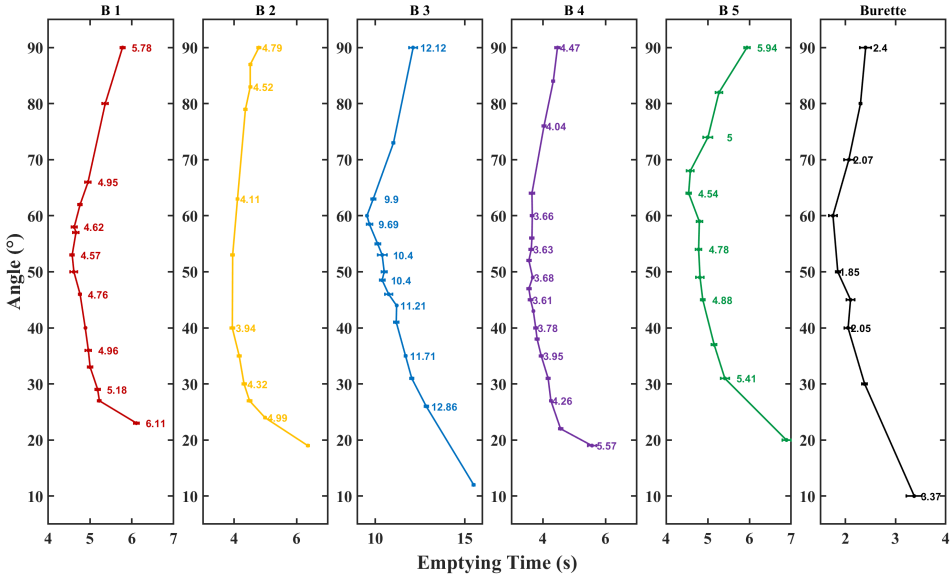

Fig. 3. The relationship between emptying time and angle for each container. From left to right are B1, B2, B3, B4, B5, and the graduated cylinder.

2.2.2 Influence of Bottle Inclination

To ignore the bottle's volume and mouth size and focus on the change in pouring angle over time, the experimental data were further processed. For each bottle, the emptying time at a 90° inclination angle was used as a reference baseline, yielding dimensionless parameters

$$\lambda = \frac{T_{emptying}(\theta)}{T_{emptying}(90)} \tag{5}$$

Where $T_{emptying}(90)$ represents the emptying time at a 90-degree tilt angle, and $T_{emptying}(\theta)$ represents the emptying time at each specific angle.

For each bottle studied, starting from a 90° tilt angle, the emptying time decreases as the angle gradually decreases. However, after reaching a certain specific angle, as the angle continues to decrease, the emptying time begins to increase. The relationship between λ and the inclination angle for each bottle is illustrated in Fig. 3. For Bottles 1, 2, and 4, which have similar shapes, characteristic angle with minimum backward time is very close. In addition, for B1 B2 and B4, the direction of the folds and the trajectories in Fig. 3 almost coincide.Bottles 3 and 5, which have more distinct shapes, show some differences in their 'specific angles,' but the pattern of first decreasing and then increasing emptying time is consistent with the previously mentioned bottles. The study also found that the tilt angle significantly impacts the emptying time; optimizing the tilt angle for the same bottle can reduce the emptying time by approximately 20 % which can be obtained in the figure 3.

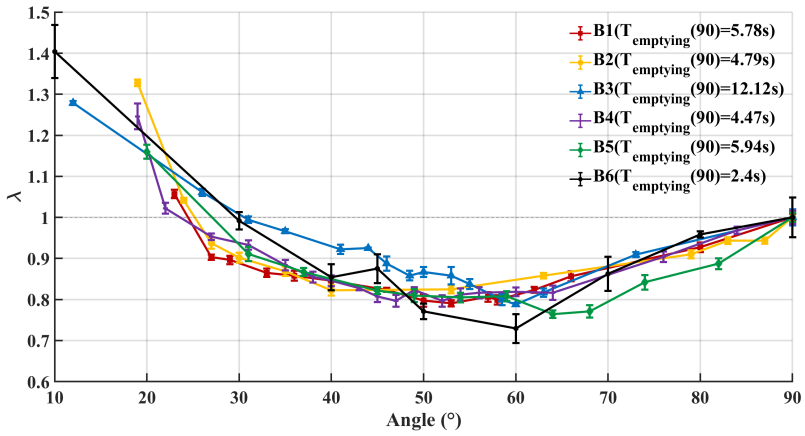

Fig. 4. Relationship curve between tilt angle and λ.

2.2.3 Influence of Surface Tension

The water emptying test with a variable surface tension (by adding liquid soap to water has been done, with the weight ratio of 1/181), but with regard to the emptying time, the obvious differences were not detected (see table 4) suggesting that surface tension plays a minimal role in the emptying time, at least for the scale that is considered in this research.

Table 2: Effect of surface tension on the emptying time T_f.

θ (°)	$T_{f,Pure\ Water}$ (s)	$T_{f,soap\ water}$ (s)
47	4.72	4.72
66	4.95	4.90
90	5.78	5.74

2.2.4 Discussion on Flowing Status

Through high-speed cameras, it was found that for B1 B2 B3 B4 and B5, which bottle mouth inside diameter were all smaller than 21mm, the process of emptying bottle can be described very clearly: first, the water clump flows out of the bottle opening under the action of gravity, while gas enters to form bubbles and rises, and then the water clump falls again. Starting from a certain time t_0, the falling of water no longer leads to the generation of bubbles, and the turbulent flow disappears, replaced by water flowing out in a very smooth manner, which is similar to the research conclusions of Geiger et al. (2012). In the subsequent analysis, the flow stage before $t < t_0$ is called the "bubble state", and the flow stage after $t > t_0$ is called the "flow dynamic". In order to characterize the influence of the inclination angle on the "bubble state" flow, a dimensionless number μ is defined as follows:

$$\mu = t_b/(t_b + t_f) \tag{6}$$

where t_b is the time used in the "bubble state", t_f is the time used in the "flow dynamic", and Figure 5 shows the relationship between μ and angle, where the black curve is obtained by a fourth-order polynomial fitting in Matlab. It can be found that as the inclination angle increases gradually, μ value generally increases, that is, the "bubble state" proportion increases. One possible reason is that a larger inclination angle will increase the liquid's pressure gradient force, which will accelerate the flow speed of the "flow dynamic" liquid and shorten the flow time of this stage, ultimately resulting in an increase in the flow time of the "bubble state" stage. Another speculation is that a larger inclination angle will reduce the remaining liquid volume at t_0,

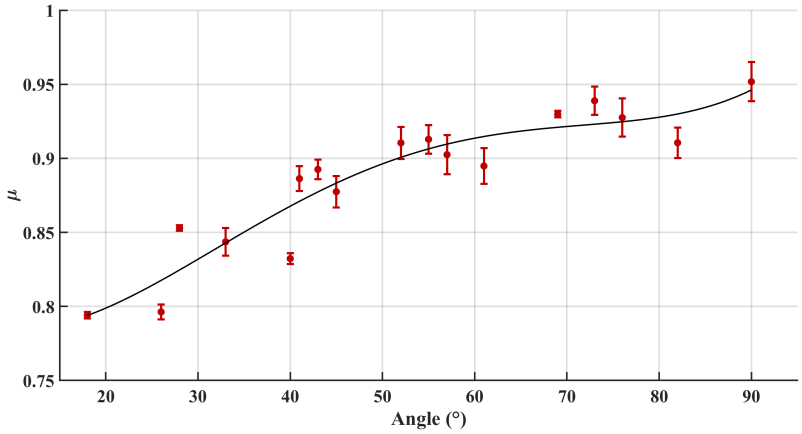

Fig. 5. Percentage of bubble state versus inclination angle.

3 Models

3.1 Modified C&S Formula

Based on C&S Formula [1], for an ideal tubular container, its emptying time at 90° is highly correlated with the shape parameter D_0,d and $L$of the container itself, as demonstrated by Eq. (1), where

$$T_{e0} = \frac{3L}{\sqrt{gD_0}} \tag{7}$$

which denotes the emptying time when the diameter of the mouth of the bottle is the same as the average bottle neck.From this can obtained:

$$Te = \frac{nL}{\sqrt{gD_0}} \left(\frac{D_0}{d} \right)^{5/2} \tag{8}$$

However, for the six different bottles used in the experiment, a large discrepancy between the prediction results of the C&S formula and the real emptying time was observed, and calculations showed that the coefficient of determination of the original C&S formula, R^2= -4.36. In order to make the C&S formula better respond to the emptying time of the real bottles, two different corrective solutions were adopted: 1. optimising the leading coefficients of Te0, i.e., changing the value of n in Eq. (8); 2. finding a new power-index relationship between $\frac{T_e}{T_{e0}}$ and $\frac{D_0}{d}$.After calculations, two new

formulas for Te are given:

$$Te' = \frac{1.8L}{\sqrt{gD_0}} \left(\frac{D_0}{d}\right)^{5/2} \tag{9}$$

$$Te'' = \frac{3L}{\sqrt{gD_0}} \left(\frac{D_0}{d}\right)^{2} \tag{10}$$

The results of the Eq. (9) and (10) are shown in Figure 6 respectively. The horizontal coordinates in the graph represent the experimental results, and the vertical coordinates represent the results of three different formulas. Among them, the R^2 of the result of Eq. (9) is 0.62 and Eq. (10) results in the R^2 of 0.85. It is easy to see that Eq. (10) has a better fit. Differences in the shape of the bottles can be considered as the reason for this change.

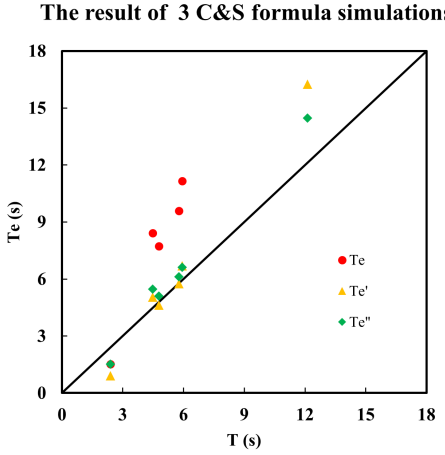

Fig. 6. Comparison of the results of the three formulas.

3.2 C&S Equation Based on Inclination Change

The variation of pouring time with inclination angle is discussed in Section 2.2.2. As can be obtained from Fig. 4, for the same inclination angle, there is a certain overall similarity between the λ for different shaped bottles, although there is a slight difference between them. To further investigate the relationship between emptying time and inclination, the dimensionless number θ' was used, where $\theta' = \theta/90$. After a quadratic polynomial fit, the equation for λ versus θ' is obtained:

$$\lambda = 1.9\theta'^2 - 2.4\theta' + 1.6 \tag{11}$$

Figure 7 illustrates the dimensionless number λ versus θ' , where the fit of Equation (11) is R^2 = 0.8672.

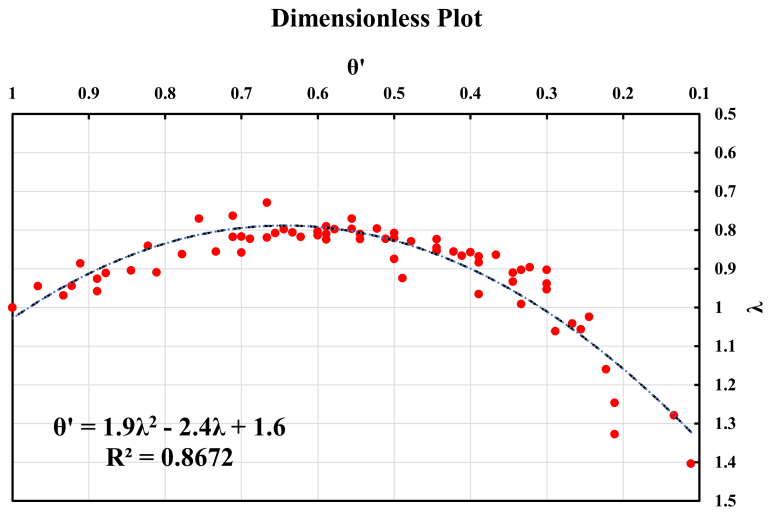

Fig. 7. Relationship between λ and θ'.

Substituting $T_{emptying}(90) = Te''$ into Eq. (5), associating Eq. (10) (11), we obtain:

$$T = [1.9(\frac{\theta}{90})^2 - 2.4\frac{\theta}{90} + 1.6]\frac{3L}{\sqrt{gD_0}}\left(\frac{D_0}{d}\right)^2 \tag{12}$$

Eq. (12) is called, the C&S equation based on inclination change.

4 CFD Simulation for Bottle Empty

The fluent model was set as transient, and the gravity acceleration in the Z direction was set as 9.81m/s^2. Fluid-water was added, boundary conditions and grid were checked. Volume of Fluid model was set, and surface tension coefficient was set as 0.072N/m. Viscous model was set as SST k-ω viscous model. The Courant number was set as 1, and the time step can be determined by dividing the local mesh size by the characteristic flow velocity, so the time step was set from 0.001 to 0.025s.

4.1 Turbulence Modeling

RANS turbulence model was used for boundary layer resolved simulation of the bottle emptying in this paper. The RANS model of choice is the SST k-ω model by Menter (1994). The SST k-ω solve two prognostic equations: the turbulence kinetic energy, k, and the specific dissipation rate, k-ω, which obtained from the following transport equations:

$$\frac{\partial \rho k}{\partial t} + \frac{\partial \rho k u_i}{\partial x_i} = \mu_t S^2 - \beta^* \rho \omega k + \frac{\partial}{\partial x_j}\left[(\mu + \frac{\mu_t}{\sigma_k})\frac{\partial k}{\partial x_j}\right]$$

$$\frac{\partial \rho \omega}{\partial t} + \frac{\partial \rho \omega u_i}{\partial x_i} = \frac{\alpha \alpha^*}{\nu_t}\mu_t S^2 - \beta \rho \omega^2 + \frac{\partial}{\partial x_j}\left[(\mu + \frac{\mu_t}{\sigma_\omega})\frac{\partial \omega}{\partial x_j}\right] + 2(1-F_1)\rho \frac{1}{\omega \theta_\omega}\frac{\partial k}{\partial x_j}\frac{\partial \omega}{\partial x_j}$$

In these equations, ρ represents density of fluid. t represents time. x_i and x_j represents axis in the i and j direction. u_i and u_j represents velocity in the i and j direction. μ_t represents turbulent viscosity. μ represents viscosity. S represents modulus of the mean rate-of-strain tensor. σ_k and σ_ω are the turbulent Prandtl numbers for k and ω, respectively. β^*, α, α^*, F_1, θ_ω are more functions and constants defined in Menter (1994).

4.2 Geometry Modeling

Geometry of the glass bottle inwall were measured according to the wall thickness and volume of the glass bottle. 3D solid model of the glass bottle were made and model quality was checked. The mesh was divided with multizone method, and the bottle mouth was set as pressure outlet boundary and the bottle body was set as wall boundary. As shown in the figure 4, two kinds of bottle models were constructed, bottle (a) is cylindrical, bottle (b) is narrow-mouth bottle with variable diameter.

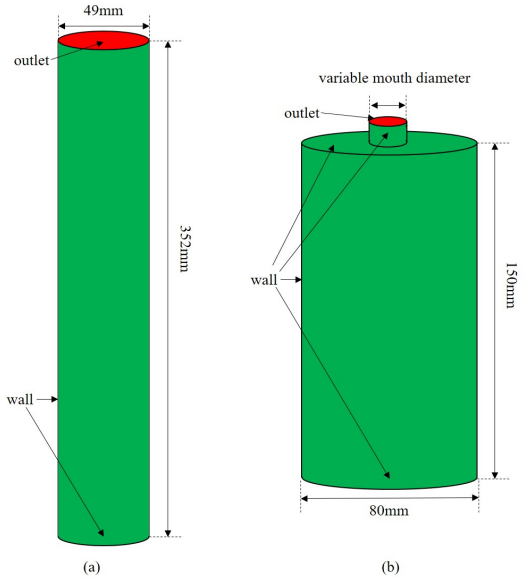

Fig. 8. Diagram of two kinds of bottle ((a) cylindrical bottle; (b) narrow-mouth bottle with variable diameter)

4.3 Convergence Test and Validation

4.3.1 Convergence Test

(1) Comparison of Mesh Generation Schemes

The 665mL cylindrical bottle (a) (diameter 49mm, height 352mm) was simulated by fluent under the upside-down condition. Different meshing and viscosity calculation schemes were set up, and the model was checked by experimental data to determine the model parameters.

Viscous model was set as SST k-ω viscous model as shown in the figure. Different mesh encryption dimensions were set, bottle empty time were calculated, and compared by experiment empty time.

Table 3: Comparison of mesh generation schemes

Case	Mesh number	Average mesh size(mm)	Time step(s)	Empty time(s)	Empty time-experiment(s)	Relative error(%)
C1	2116	17.7	0.035	2.500	2.400	4%
C2	5658	10.8	0.022	1.950		-19%
C3	30475	4.7	0.009	2.325		-3%
C4	51590	3.6	0.007	2.100		-13%
C5	126083	2.3	0.005	2.225		-7%
C6	255750	1.6	0.003	2.440		2%
C7	518830	1.1	0.002	2.500		4%

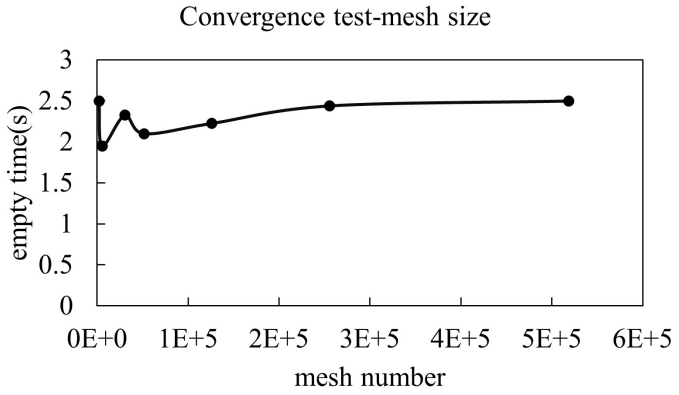

Fig. 9. Diagram of the convergence test on mesh size

It can be seen that the case C6 converges and has the smallest relative error, so average partitioning size was set as 1.6mm.

(2) Viscous model

Based on the Case C6, using the fluent meshing method with time step of 0.003s, comparing SST k-ω and laminar viscosity model, bottle empty time was calculated, and contrasted with experiment empty time.

Table 4: Comparison of viscous model schemes

Case	Viscous model	Empty time(s)	Empty time -experiment(s)	Relative error(%)
C6	SST k-ω	2.440	2.400	2%
C6 laminar	laminar	2.175		-10%

It can be shown that the relative error of Case C6 is the smallest, so SST k-ω viscous model was used.

4.3.2 Validation

Empty experiments were performed on a 665mL cylindrical glass bottle (49mm in diameter and 352mm in height) with different angles. Since the opening direction of the glass bottle geometry was the positive half axis of the Z axis, the acceleration of gravity at different angles was set and the bottle emptying time was calculated, and contrasted with experiment empty time.

Table 5: Bottle empty time comparison with different incline angle

incline angle(°)	empty time(s)	empty time -experiment(s)	relative error(%)
90	2.44	2.40	4.2
80	1.95	2.30	-13.0
70	1.78	2.07	-11.8
60	1.63	1.75	-4.3
50	1.59	1.85	-12.2
45	1.59	2.10	-22.6
40	1.61	2.05	-19.5
30	1.71	2.38	-26.5
10	2.51	3.37	-23.6

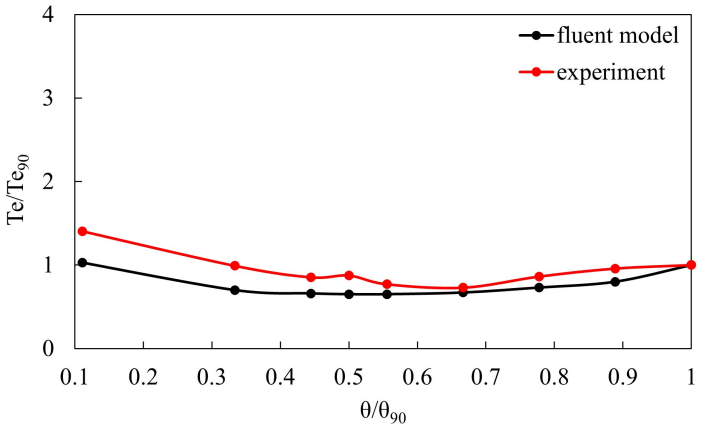

Fig. 10. Diagram of the relationship between relative empty time and relative incline angle

Since the end criterion of the empty bottle experiment is judged by no continuous flow which may last for several seconds, and in CFD simulation, 1-10 drops of water per unit time are generally used as the judgment standard, which will lead to large errors, as shown in table 5.

4.4 Results and Discussion

As can been seen in fluent model, there is no flow for d<5mm due to surface tension effects. In the region of counter flow (outlet diameter d>21 mm), the outlet provides enough space so that water and air can pass each other simultaneously in the in- and out- flow directions. In the region of oscillatory flow (d is between 5 and 21 mm), flow pattern is characterized by four (cyclic) stages: liquid downflow, bubble rise, repressurization, and refill, which is similar to flow pattern analysis proposed by Geiger et al. (2012). According to fluent test, relative maximum flow rate had an exponential relationship with relative bottle mouth diameter as shown in figure 7.

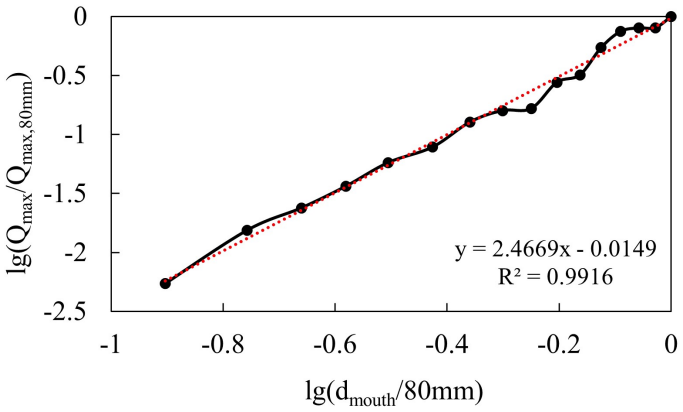

Fig. 11. Diagram of the relationship between relative maximum flow rate and relative bottle mouth diameter

5 Conclusion

For realistic bottles, their bottle calibre and pouring time show a certain correlation, and for bottles of similar volume, the larger the bottle calibre, the faster the flow emptying time.

A very consistent relationship was found between the change in inclination angle and the pouring time. Overall, the pouring time increases and then decreases as the angle becomes progressively smaller, while the shortest pouring time occurs between 40° and 60°, which is about 80% of the pouring time at 90°.

For surface tension, the effect of its change on the inversion time was not obvious in the experiments.

For the flow regime, the flow voiding process is divided into ”bubble state” and ”flow dynamics”, and the percentage of the ”bubble state” phase decreases as the tilt angle decreases.

Based on empty bottle experiment and fluent simulation, three different flow regimes with different bottle mouth diameters were analyzed: no flow, counter flow, and oscillatory flow. Exponential relationship between relative maximum flow rate and relative bottle mouth diameter was obtained by regression method.

Acknowledgement

Shenglin Yue, Xiaotian Dong, Rongtian Na and Zhixin He contributed equally to this work and should be considered co-first authors.

References

[1] Clanet, C. and Searby, G. (2004) 'On the glug-glug of ideal bottles', *Journal of Fluid Mechanics*, 510, pp. 145–168. Available at: https://doi.org/10.1017/S002211200400936X.

[2] Davies, R.M. and Taylor, S.G. (1988) 'The mechanics of large bubbles rising through extended liquids and through liquids in tubes', in Dynamics of Curved Fronts. Elsevier, pp. 377–392. Available at: https://doi.org/10.1016/B978-0-08-092523-3.50041-1.

[3] Kenton, Z.A., Neufeld, J.A. and Huppert, H.E. (2012) 'Emptying Bottles: A Study of Glugging'.

[4] Mayer, H.C. (2019) 'Bottle Emptying: A Fluid Mechanics and Measurements Exercise for Engineering Undergraduate Students', Fluids, 4(4), p. 183. Available at:https://doi.org/10.3390/fluids4040183.

[5] Mer, S. et al. (2019) 'Emptying of a bottle: How a robust pressure-driven oscillator coexists with complex two-phase flow dynamics' .Available at:https://doi.org/10.1016/j.ijmultiphaseflow.2019.05.012.

[6] Whalley, P.B. (1991) 'Two-phase flow during filling and emptying of bottles', International Journal of Multiphase Flow, 17(1), pp. 145–152. Available at: https://doi.org/10.1016/0301-9322(91)90076-F.

[7] Rohilla, L. and Das, A.K. (2020) 'Fluidics in an emptying bottle during breaking and making of interacting interfaces', *Physics of Fluids*, 32(4), p. 042102. Available at: https://doi.org/10.1063/5.0002249.

[8] Silva, L.F.L.R., Damian, R.B. and Lage, P.L.C. (2008) 'Implementation and analysis of numerical solution of the population balance equation in CFD packages', *Computers Chemical Engineering*, 32(12), pp. 2933–2945. Available at: https://doi.org/10.1016/j.compchemeng.2008.03.007.

[9] Schwefler, C. (2021) *Analytical, Numerical, and Computational Methods to Analyze the Time to Empty Open, Closed, and Variable-Topped Inverted Bottles*. California Polytechnic State University. Available at: https://doi.org/10.15368/theses.2021.88.

[10] Geiger, F., Velten, K. and Methner, F.J. (2012) '3D CFD simulation of bottle emptying processes', *Journal of Food Engineering*, 109, pp. 609–618. Available at: https://doi.org/10.1016/j.jfoodeng.2011.10.008.